

Sensor and Simulation Notes

Note 334

October 15, 1991

CANONICAL EXAMPLES OF REFLECTOR ANTENNAS FOR
HIGH POWER MICROWAVE APPLICATIONS

Y. Rahmat-Samii and D. W. Duan
Department of Electrical Engineering
University of California, Los Angeles
Los Angeles, CA 90024-1594

D. Giri
Pro-Tech
Lafayette, CA 94549-3610

ABSTRACT

The suitability of various radiating systems for generating a directive high power microwave (HPM) beam is investigated. It is concluded that offset reflector antenna systems are well suited for this purpose. An HPM reflector antenna may consist of one or two reflectors that are illuminated by single or array feeds. To accurately predict the performance of an HPM reflector antenna, a versatile analysis scheme is used to compute the fields of an array feed with general configurations, and the diffraction techniques of Physical Optics (PO) and Physical Theory of Diffraction (PTD) are applied to analyze reflectors of conic or shaped surfaces. Design examples of offset dual-reflector antennas for HPM applications are presented. Analysis results are shown with emphasis on both the near-field and far-field radiation characteristics. Applications of optimization (mathematical programming) techniques to the synthesis of HPM reflector antenna systems are discussed, and examples are given to demonstrate its effectiveness.

CLEARED FOR PUBLIC RELEASE
PL/PA 15 JAN 97

PL 96-1157

Preface

This work was performed jointly by Dr. Y. Rahmat-Samii and D. W. Duan (Department of Electrical Engineering, University of California, Los Angeles) and Dr. D. V. Giri (Pro-Tech), and was sponsored by the U. S. Army.

Contents

Section	Page
I. Introduction	3
II. Antenna systems for directive HPM beams	5
III. Analysis of HPM reflector antenna systems	8
IV. Synthesis of HPM reflector antenna systems	12
V. Design examples	16
VI. Conclusion	33
Reference	34

I Introduction

In the context of generating directive HPM beams, several problems arise that are not of consequence at lower power levels. It is generally regarded that peak power levels above 100 MW are considered as "high power" in the HPM context. In designing an antenna system for HPM application, one has to consider the following steps in detail, viz., (1) identify all of the critical antenna issues arising from the high power levels, (2) study the feasibility of different antenna systems and choose a suitable system, (3) develop mathematical models and computational tools required for the synthesis, (4) perform antenna analysis leading to predicted performance, (5) design low-level testing experiments and finally (6) testing of the high power system. In carrying out these steps, some of the assumptions and requirements consist of: (i) pulse mode operation with peak power in the 1 to 10 GW range and pulse width in the range of 0.2 to $1\mu s$, (ii) 1 to 3 GHz frequency of operation with 1 to 20 Hz pulse repetition frequency. The radiating system requirements typically are 30 to 40 dB antenna gain with moderate side lobe levels and beam scanning capabilities.

A schematic of an antenna system for HPM radiation is shown in Fig. 1. It consists of an HPM source from which the power is extracted and carried in evacuated waveguides, followed by beam forming network (e.g. phase shifting, combining or splitting of waveguides etc.) that leads into a feed array where proper interfaces are placed to avoid high-voltage breakdown. In this paper, some representative configurations will be considered for various radiating systems in the context of high power levels. A conclusion from this investigation is that offset reflector antennas are well suited for generating HPM beams.

Based on this conclusion, a recent advance in the analysis and synthesis of reflector antennas for HPM applications will be described. The development of advanced

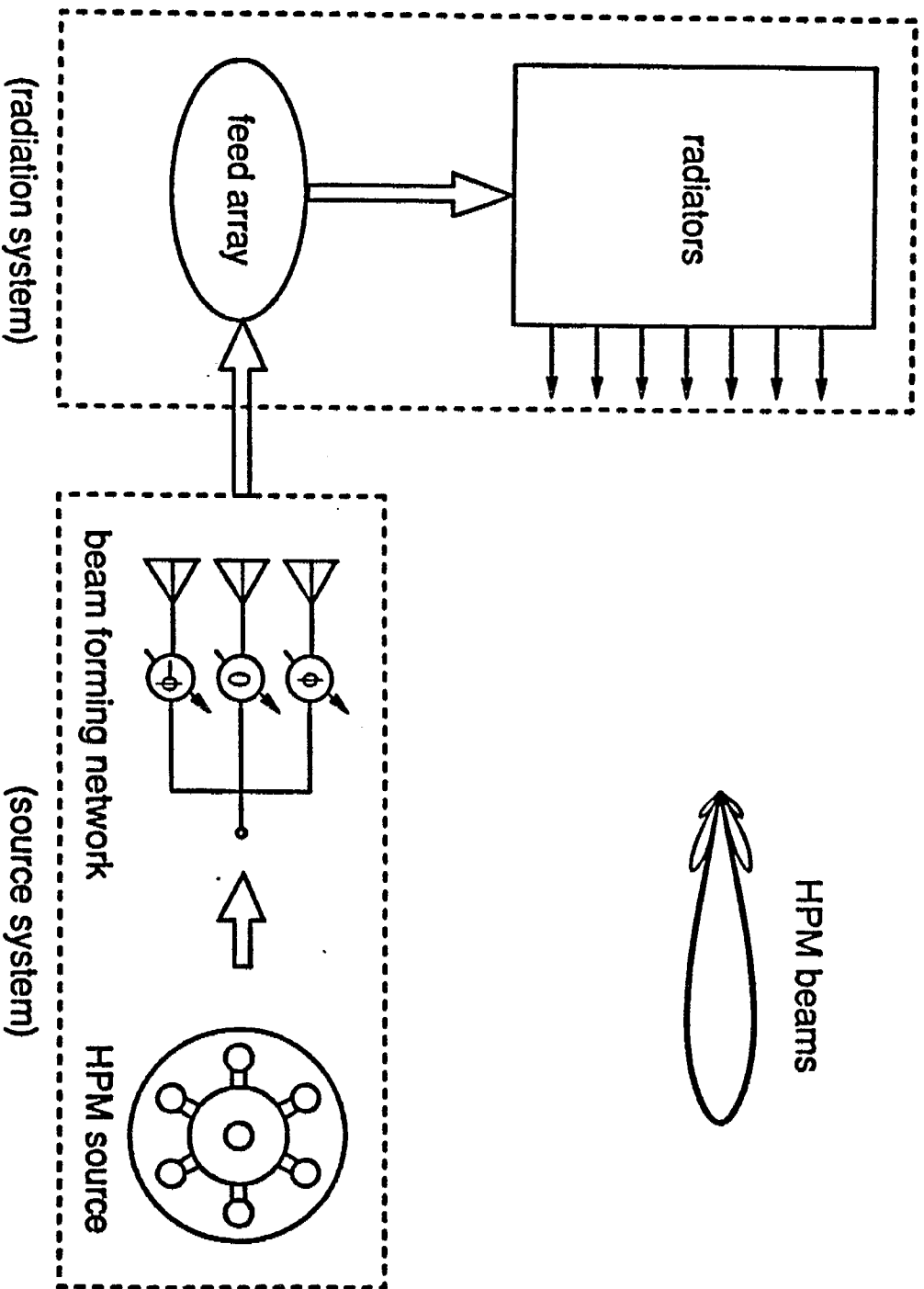


Figure 1: High power microwave antenna system schematics.

diffraction analysis schemes is motivated by the need of accurate evaluation of the performance of HPM reflector antennas. Accurate diffraction analysis results are very important in determining, for example, (a) whether the specifications on the far field radiation patterns are fulfilled, (b) whether the near field strength exceeds the safe margin for air breakdown, and (c) a safe range for personnel exposure. In HPM reflector antennas, HPM sources and the air breakdown problem may impose restrictions on the design of feeds, which can result in undesirable feed radiation characteristics. This necessitates the development of advanced synthesis methodology which can be used to effectively improve (optimize) the antenna performance under undesirable feed characteristics. Specifically, for the analysis, a versatile scheme is used to compute the fields of an array feed with general configurations, and the diffraction techniques of Physical Optics (PO) and Physical Theory of Diffraction (PTD) are applied to analyze reflectors of conic or shaped surfaces. For the synthesis, optimization techniques are employed to search for values of system parameters that optimize the antenna performances. This general analysis/synthesis approach will be demonstrated by design examples of HPM dual-reflector antennas which may have shaped reflectors. Analysis results will be presented with emphasis on both the near-field and far-field radiation characteristics.

II Antenna systems for directive HPM beams

We start with the assumption that the power from the HPM source is available from a number $N(\geq 1)$ of evacuated waveguides. A list of possible radiators are: (a) dipole antenna, (b) log-periodic antenna, (c) leaky pipe or slotted waveguide antenna, (d) antenna array of horn elements, (e) dielectric lens antenna and (f) reflector antenna. The performance characterization of these classical antennas are

obtainable from well established theoretical and experimental data [1, 2]. Using the above radiating elements, many types of radiating systems can be considered in meeting the present requirements. However, one has to individually consider their suitability for high power applications.

A Dipole antenna

A conical shaped dipole antenna has been considered and used for radiating a transient pulse in the nuclear electromagnetic pulse (NEMP) context [3]. However, it is unsuitable for generating a directive HPM beam. It has a null in the axial direction and an isotropic pattern in the azimuthal plane.

B Log-periodical antenna

The primary reason for not using a log periodical antenna in the HPM area is that one is faced with the problem of driving the input port of the antenna with a high power pulse. It is basically a problem of bringing the high power into a pair of terminals. This antenna has some very desirable properties and well-suited for certain low power applications, but is relatively less efficient compared to other antennas for HPM such as reflectors.

C Leaky pipe or an array of slotted waveguides

It is in principle possible to produce a main lobe at some prescribed direction by using non-resonant radiating slots in waveguides. However, the power that can be efficiently radiated from a single slot is of the order of 1 MW. This suggests that one requires hundreds or even thousands of slots to radiate several GW of HPM. Such antenna systems are suited in low-power flush-mounted aerodynamic applications and can be ruled out in HPM applications.

D Array of horn elements

Circular aperture antennas [4] formed by an array of horns could also be considered. The fields in each horn can be uniform in phase and amplitude. The disadvantage is that it takes many horns to produce a large aperture plane in terms of wavelength dimensions. Furthermore, it may be impractical to obtain beam scanning by mechanical rotation.

E Dielectric lens antenna

A single large dielectric lens can be built to radiate a narrow beam in the far-field. Alternatively, one can think of an array of small dielectric lenses, wherein each lens is fed by its own horn to produce a narrow beam in the far-field. Both of these schemes appear impractical in terms of obtaining a large aperture (several tens of wavelengths in size), which is easily accomplished by using reflector antennas.

F Reflector antennas

A single large reflector fed by a single horn or by a cluster-feed arrangement is an efficient radiator to produce a directive beam in the far-field, if no beam steering is required. It could be impractical to mechanically rotate a large (several meters in diameter) reflector to achieve beam steering. Furthermore, due to the complexity of the feed system, it is assumed that the feed system can not be easily moved to generate scanned beams. An excellent alternative is to use a dual-reflector antenna e.g. a Cassegrain system where the smaller subreflector is a hyperboloidal or shaped surface, and the larger main reflector is a paraboloidal or shaped surface. Offset Cassegrain system can then minimize aperture blockage and help in beam steering. Beam steering is feasible by keeping the main paraboloidal reflector fixed and moving the smaller hyperboloidal subreflector.

We have also investigated the hardware requirements in each of the above radiating systems. The comparisons of various antenna systems lead us to recommend the use of an offset Cassegrain fed by one or more pyramidal horns. At low power levels, electronic steering has been successfully employed. The electronic steering in general consists of target sensing, computing propagation delays (equivalently phase shifting) for individual elements and adjusting for these delays by computer controlled delay circuits. This method is impractical at high power levels, where dynamic phase shifting or delay line technology for evacuated waveguide runs is yet to be developed and refined. For the present, mechanical steering by moving a small subreflector appears to be an efficient option.

III Analysis of HPM reflector antenna systems

To choose an appropriate reflector antenna configuration for HPM applications, the following considerations must be taken into account. (i) To avoid aperture blockage and facilitate efficient power delivery, offset geometry will be adopted. (ii) In order to satisfy specifications on radiation patterns, shaped dual- or single-reflector antenna may have to be used. (iii) The air breakdown problem discourages the use of Gregorian-like dual-reflector antennas. (iv) To extract and convey the power generated by HPM sources to the reflectors, the feeding system may consist of an array feed. In particular, it is possible that some topological or physical constraints set by the sources may cause undesirable feed characteristics.

Based on these considerations, the general geometry of HPM reflector antenna systems is depicted in Fig. 2 and 3 for dual- and single-reflector antennas respectively. Performance evaluation of such HPM reflector antenna systems will be discussed in this section.

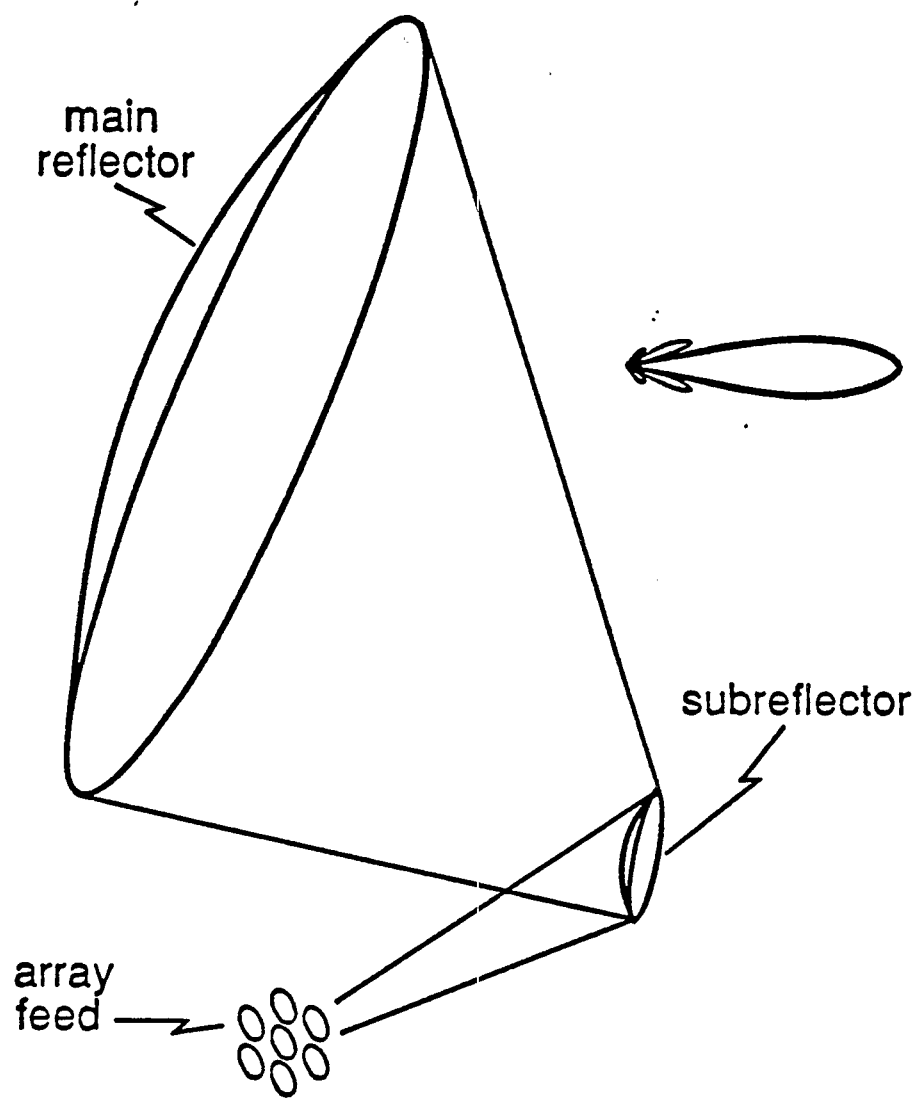


Figure 2: HPM reflector antenna geometry: an offset shaped dual-reflector antenna fed by a generally configured array feed.

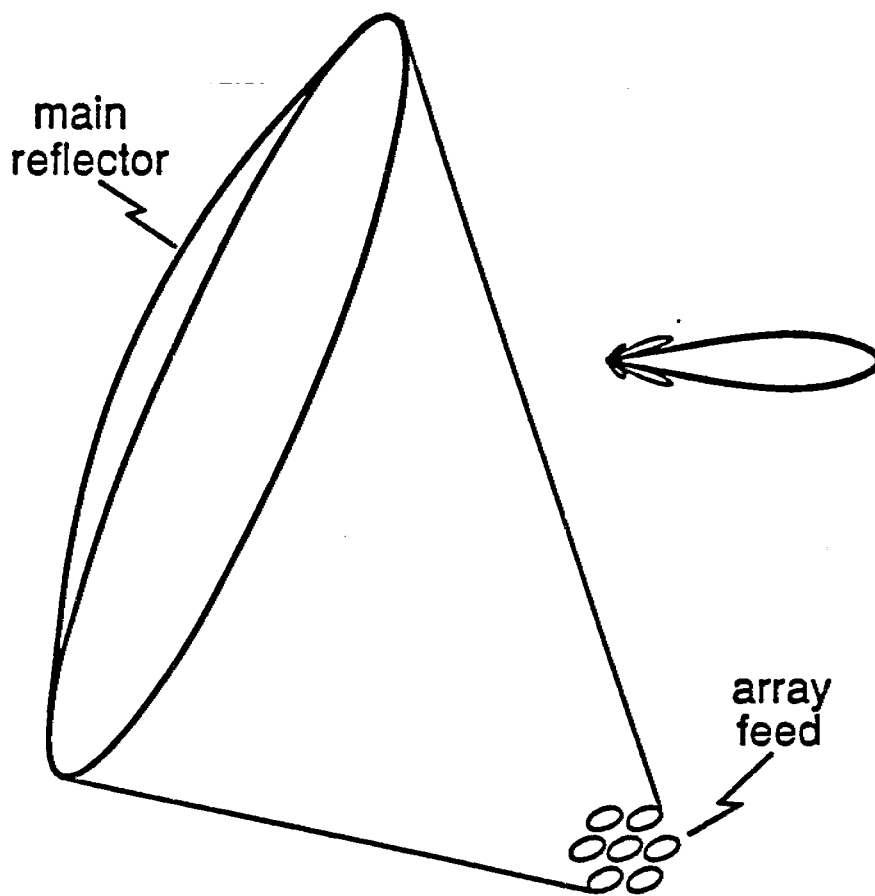


Figure 3: HPM reflector antenna geometry: an offset shaped single-reflector antenna fed by a generally configured array feed.

A Array feed

The feeding system of an HPM reflector antenna must be capable of delivering the power generated by the HPM sources to the reflectors. The combination of the HPM source characteristics and the power delivering mechanisms may impose undesirable restrictions on the feed configurations. Therefore, one must allow for a versatile design approach so that various parameters can be adjusted to produce the desired radiation patterns with appropriately shaped reflectors. Under these considerations, the feeding system of an HPM reflector antenna may consist of a cluster of feeds which have complicated configuration. In order to handle such general array configurations, a computer program has been developed to calculate the vector E-field and H-field at near and far field observation points. The radiation from a single feed element can usually be characterized with reasonable accuracy using analytical method, numerical computation, measured data or their combinations. However, in considering the near field effect of the array feed and the air breakdown problem, accurate models such as the aperture field method for sectoral horns or spherical wave expansions must be used.

B Reflectors

There are many methods that can be applied to analyze the radiation from the reflectors [2]. In order to obtain accurate prediction, the diffraction techniques Physical Optics (PO) and Physical Theory of Diffraction (PTD) will be used in the HPM applications. PO can accurately predict the field in the main beam region and near side lobes. In the far-angle or cross-polarized field predictions, however, the reflector edge diffraction may become important. In this situation, PTD techniques should be included to complement PO for edge diffraction effect. In PTD, the PO fields

are modified by a fringe field that is obtained by an one-dimensional integration of the equivalent edge currents along the reflector edge. This modification is efficient because the computation time is dominated by the two dimensional PO integration. The PTD techniques of interest are (a) Michaeli's equivalent edge currents [5], (b) Mitzner's incremental length diffraction coefficients (ILDC) [6], and (c) Ando's modified physical theory of diffraction [7], which are modifications of Ufimtsev's PTD [8]. These techniques have been formulated in a unified manner for thin scatterers and compared using a circular disc and a dipole feed [9]. In this paper, Michaeli's equivalent edge currents will be used in the PTD diffraction analysis.

A computational algorithm has been developed to perform the PO/PTD analysis on both single- and dual-reflector antennas. This algorithm puts no restrictions on the relative positions and orientations of various antenna components. The observation points can be in the near- or the far-field of the antennas. Near-field analysis is important for HPM antennas not only because of the near-field effect of the feeds, but also for air breakdown considerations. The reflector surfaces can be (a) the conical-section surfaces such as those used in Cassegrain, Gregorian and paraboloidal antennas, or (b) shaped surfaces. The two-dimensional PO integration is performed efficiently using Gaussian quadrature formulas. Many antenna configurations have been used to test this program and comparisons on various field characteristics have been conducted.

IV Synthesis of HPM reflector antenna systems

Optimization (mathematical programming) techniques have become more and more indispensable in the design of modern antennas. This increasing popularity is attributed to the fact that the computing environment provided by optimization tech-

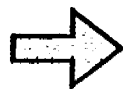
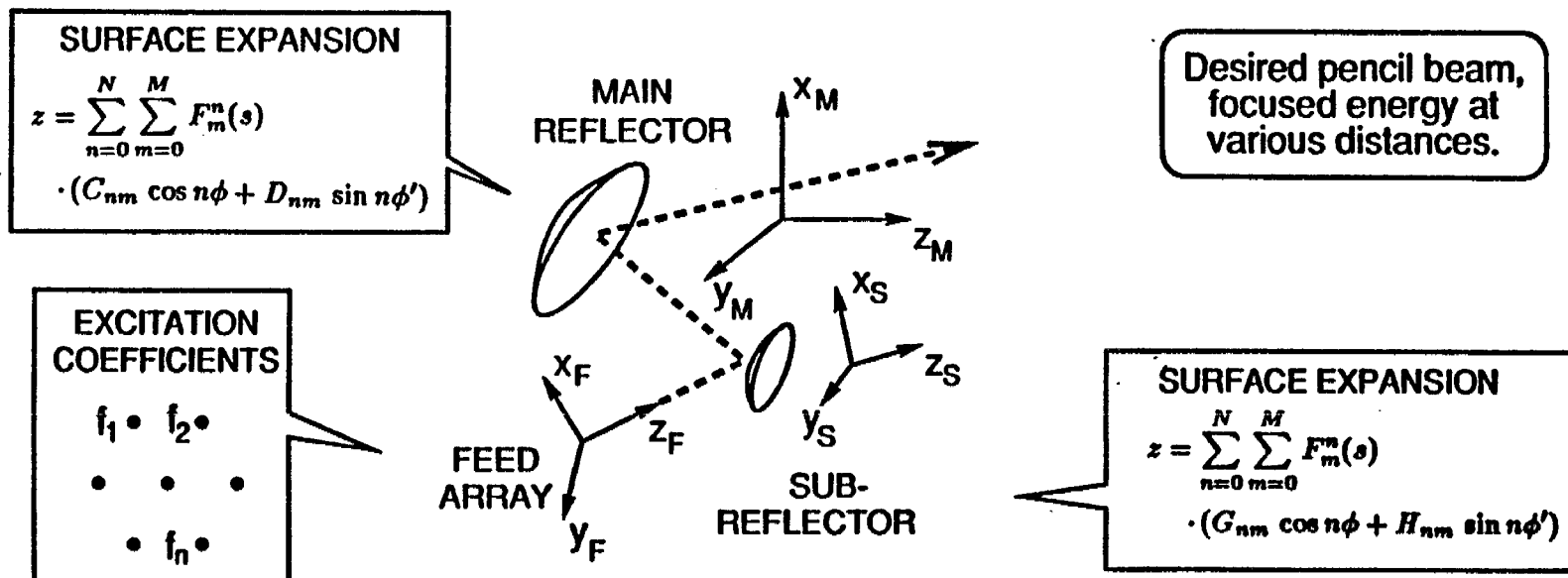
niques (a) encourages general and flexible approach to antenna designs problems, (b) provides feasible and reliable computational schemes, and hence (c) enlarges the scope of antenna designs. General picture of the theoretical aspect of optimization can be found in reference [10]. Reference [11] provides much insight and hints in the application and implementation of optimization algorithms.

The two major steps in applying optimization techniques to the diffraction synthesis of array fed dual-reflector antennas for HPM applications is shown in Fig. 4 and 5 respectively. The goal of synthesis is to improve the antenna efficiency and produce the desired secondary pattern in the presence of undesirable radiation characteristics of the feed system. In the first step, the antenna system to be optimized is parameterized. For example, the reflector surfaces are expanded in terms of orthogonal functions over an elliptical (or circular) region, and the expansion coefficients will be adjusted by an optimizer to achieve the desired antenna performance. Any other parameters, such as the excitation coefficients of the array elements and antenna geometrical dimensions can also be used as optimization variables. In the second step, optimization techniques are applied to search for a set of optimized variables. In each iteration of this procedure, radiation characteristics of interest are computed by the PO/PTD analysis. Difference between these computed values and the desired values are indicated by an object (cost) function. When the value of this function is satisfactorily minimized, a set of optimized variables have been found and the synthesis procedure ends. Otherwise, a new set of trial variables are searched by the optimizer, and used in the next iteration.

Advantages of using this optimization approach for antenna synthesis are summarized in the following. (i) No more approximations than those assumed in the analysis are needed. (ii) Accurate diffraction analysis is performed simultaneously

STEP 1: PARAMETERIZE AN ANTENNA SYSTEM

14



THE COEFFICIENTS C_{ij} , D_{ij} , G_{ij} , H_{ij} AND f_n ARE TO BE ADJUSTED BY AN OPTIMIZER (IN STEP 2).

Figure 4: Diffraction synthesis of array fed reflector antennas using optimization techniques – step 1.

STEP 2: APPLY OPTIMIZATION TECHNIQUES

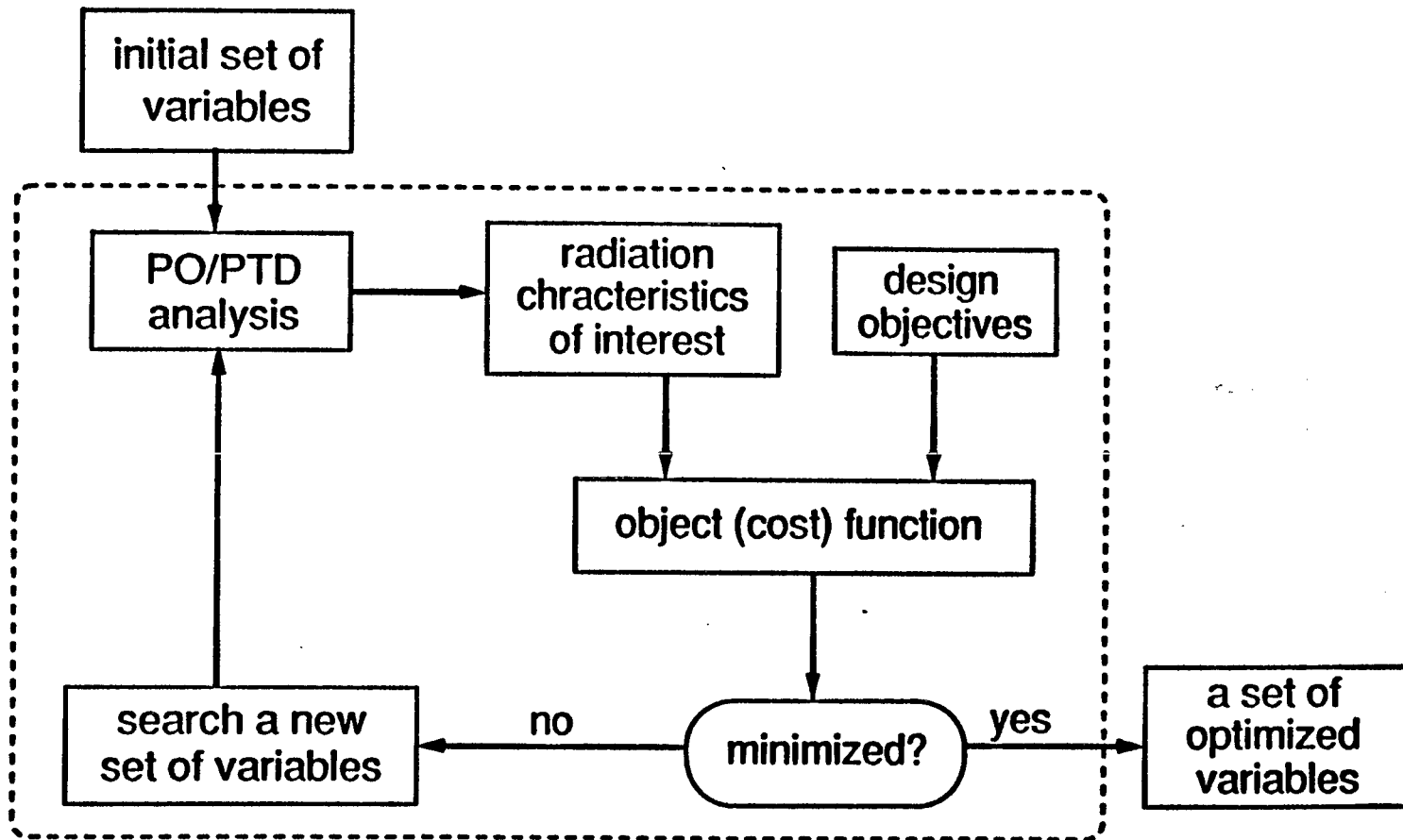


Figure 5: Diffraction synthesis of array fed reflector antennas using optimization techniques – step 2.

Table 1: Important design parameters for the example reflector antennas.

Frequency	3 GHz
Power	1 GW
Gain	30 to 40 dB
Side lobe levels	Moderate

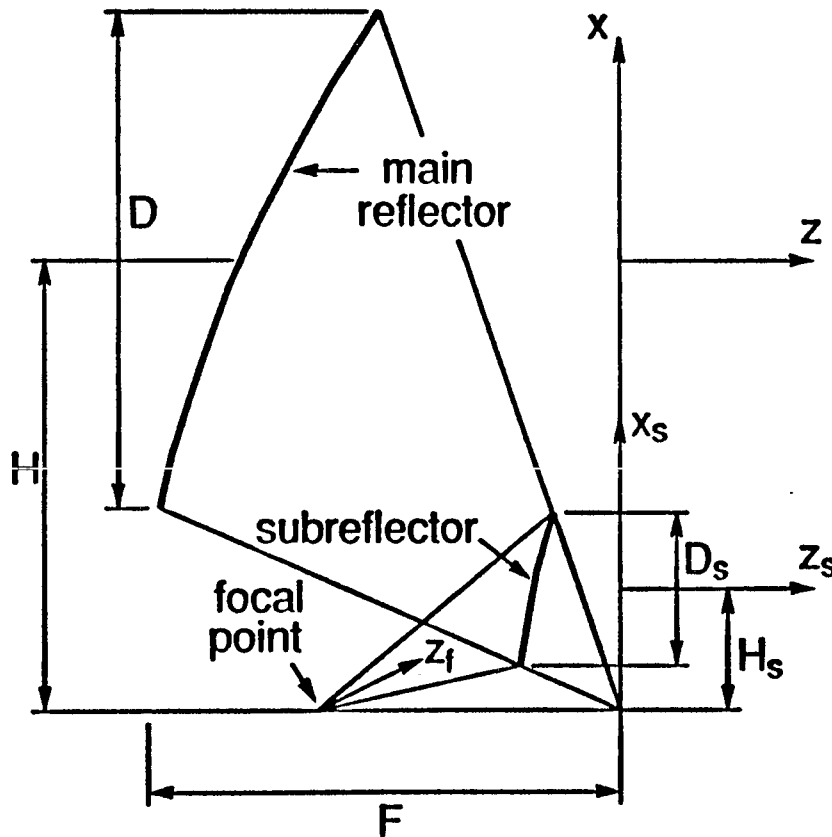
with synthesis. (iii) Antennas with general configurations can be synthesized and any antenna parameters can be optimized. (iv) Using properly designed object function, it is possible to optimize the antenna performance over a frequency band and/or a range of scanning angles. For reflector antennas, in particular, this optimization synthesis methodology is applicable to antennas with array feeds and/or aperture type feeds (horns, for example). The classical geometrical synthesis procedure may not be applicable to these cases.

V Design examples

In this section, representative dual-reflector antennas will be designed and analyzed using the methodology described in previous sections. For convenience, important design parameters for these examples are summarized in Table 1. Examples on single-reflector antennas will not be presented because, as mentioned earlier, mechanical beam steering by moving a large main reflector is impractical. Furthermore, only Cassegrain type dual-reflector antennas with conic or shaped reflectors will be considered because the focusing feature of Gregorian type antennas can cause serious air breakdown problems. Reflector antenna configurations that will be considered are summarized in Table 2.

A Reflector geometry

The antenna geometry is depicted in Fig. 6. This geometry is obtained by assuming



frequency: 3 GHz

main reflector:

paraboloidal or shaped

$$D = 33\lambda$$

$$F = 33\lambda$$

$$H = 30\lambda$$

subreflector:

hyperboloidal or shaped

$$D_s = 10.2\lambda$$

$$H_s = 8\lambda$$

eccentricity = 3

magnification = 2

feed system:

single horn or horn array

Figure 6: Antenna geometry used in the design examples.

Table 2: Reflector antenna configurations considered in the design examples.

Antenna	Offset dual-reflector antenna
Main reflector	Paraboloidal or shaped
Subreflector	Hyperboloidal or shaped
Feed system	Single pyramidal horn or array pyramidal horn feed

a paraboloidal main reflector and a hyperboloidal subreflector, and tracing a circular cone of rays emanating from a focal point of the hyperboloidal subreflector. The resultant main reflector has a circular aperture, and the subreflector has an elliptical aperture. For the sake of less spill-over loss and potentially better scanning performance, however, the elliptical aperture of the subreflector will be extended to a circular one that uses the major axis of the original ellipse as its diameter (D_s). It is important to mention that, although the antenna geometry is generated by conic reflectors, these reflectors will later be shaped to compensate for the undesirable radiation characteristics of the feed horn(s). Scanning performance of the designed antennas will not be discussed in this paper. However, it has been taken into consideration in the determination of some of the geometrical parameters.

The diameter of the main reflector ($D = 33\lambda$) is determined by the required antenna gain specification as described in the introduction. A circular aperture of this size has an ideal directivity of 40.3 dB. If an ideal point-source feed is used to produce an edge illumination taper about -11 dB [2], an efficiency of 72 % (-1.4 dB) can be achieved using conic reflector surfaces. This means that the highest achievable directivity is approximately 38.9 dB, which is within the specified range and allows a sufficient tolerance for other losses.

An F/D value of unity is selected by compromising the following facts. A larger focal length F will result in a smaller subtended angle of the subreflector, and this demands a higher directivity for the feed horn(s). However, when the horn aperture

is enlarged to produce higher gain, more power can go into the grating lobes which are far away from the capture of the subreflector. A smaller F will reduce the scanning capability of the antenna system, and cause more significant near field effect of the feed.

The offset height H is chosen so that subreflector blockage in the geometrical optics (GO) sense is avoided, and the cross-polarization field caused by the offset geometry is maintained at low levels. The eccentricity of the hyperboloidal subreflector is obtained by making a compromise between the scanning performance and the subtended angle of the subreflector. The subreflector axis is not tilted with respect to the main reflector axis because, in this application, suppression of cross-polarization fields is not of primary concern and untilted axis results in simpler mechanical construction.

B Horn feeds

For purpose of demonstration, only fundamental mode pyramidal horn(s) will be considered as the feed for the designed antennas. Other types of horns such as multi-mode pyramidal horns and conical horns may potentially be properly designed to obtain HPM feeds with improved radiation characteristics.

The block schematic of an HPM single horn feed system is depicted in Fig. 7. Detailed descriptions for the components in this feed system can be found in [12], and are summarized in the following. In order to avoid air breakdown at high power levels, the waveguides that carry the microwave power out of a suitable source (Xatron) are evacuated. To increase the breakdown field strength in the vicinity of the horn outlets, a polyethylene container holding the SF_6 (sulfur hexa fluoride) gas may be used as an interface between vacuum and the outside air. The extent of the SF_6 container is determined by the criterion that field strength everywhere inside or

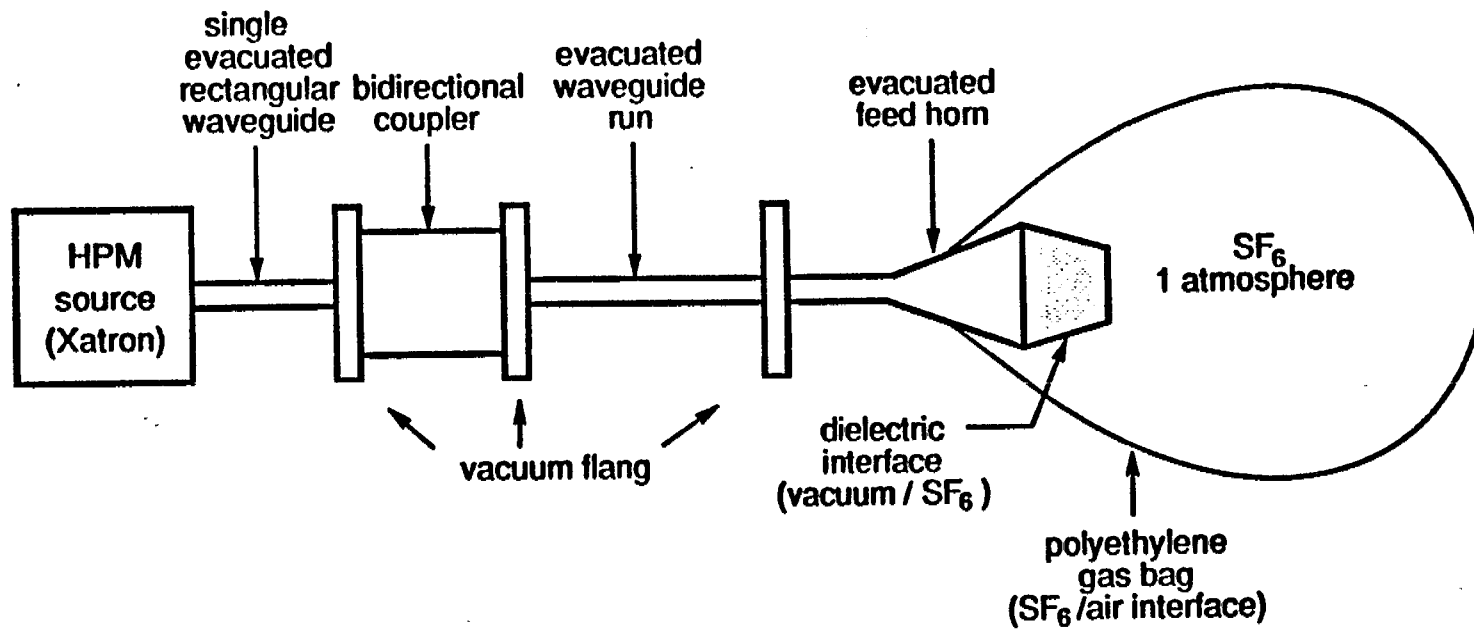


Figure 7: Elements of a single waveguide feed system.

Table 3: Design of a single pyramidal horn feed.

a	0.8636λ
b	0.4318λ
A	4.7041λ
B	4.4718λ
Horn length	15.0548λ
Phase error	15 % (H-plane), 15 % (E-plane)
Flare angle	7.27° (H-plane), 7.64° (E-plane)

outside the container must not exceed the respective breakdown level. A dielectric interface between vacuum and the SF_6 gas is situated at the horn aperture. Notice that if horn array is used instead of a single horn, more complicated power extraction mechanism and power dividing network must also be considered in addition to the simple block schematic shown in Fig. 7.

Let us conservatively take 1 MV/m as the safe margin for the field strength in the air. This level will be increased to about 3 MV/m by 1 atmosphere SF_6 gas. Using these assumptions, an important guideline in the feed design is to make the peak field strength in the horn aperture less than 3 MV/m, and the field strength everywhere outside the SF_6 container is less than 1 MV/m. This guideline will demand a minimal horn aperture size for a given power level. Two feed designs will be described in the following. One is a single-horn feed, and the other is a 7-horn array feed. All these horns are based on the waveguide WR340, and are designed for a power level of 1 GW at 3GHz.

The design of a single-horn feed is summarized in Table 3, and the geometry is shown in Fig. 8. Notice that the resultant horn aperture area is larger than $20.55\lambda^2$, which is the minimal value obtained by considering a peak aperture field of 3 MV/m at 1 GW power level. The far field distance for this horn is more than 50λ away from the horn aperture. This means that if this horn is used as the feed for our

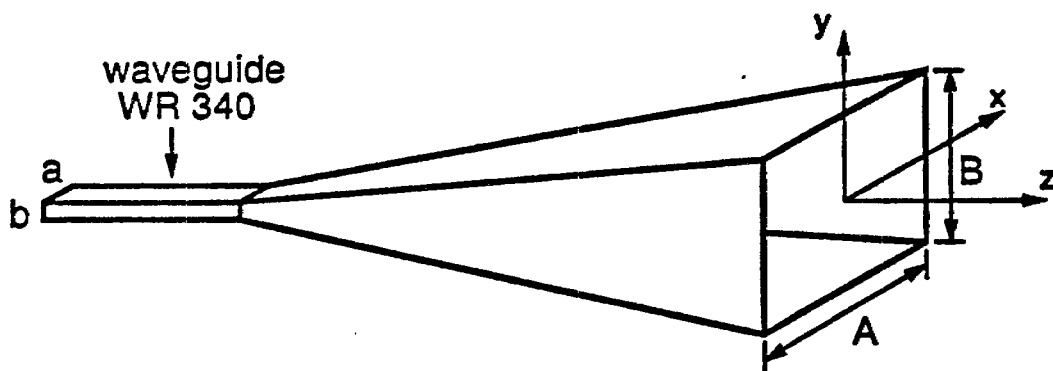


Figure 8: A single pyramidal horn feed.

Table 4: Design of a 7 pyramidal horn feed.

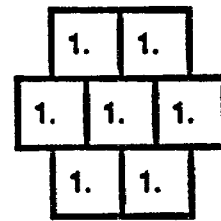
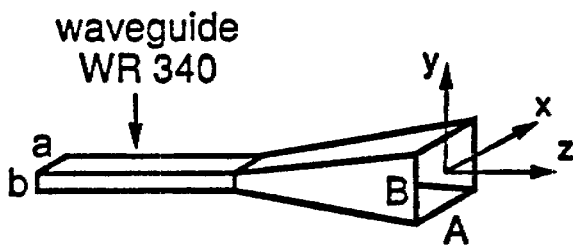
a	0.8636λ
b	0.4318λ
A	1.7780λ
B	1.7734λ
Horn length	4.9565λ
Phase error	4 % (H-plane), 6 % (E-plane)
Flare angle	5.27° (H-plane), 7.71° (E-plane)

example antennas, the subreflector will be in the near field of the horn.

An advantage of using a horn array is that the horn length can be significantly reduced. For example, the 7-horn array is assumed to be uniformly excited in order to achieve a shortest maximal horn length. The design of a 7-horn array is summarized in Table 4, and the geometry is shown in Fig. 9. Notice that the resultant element horn aperture area is larger than the required minimal value of $2.94\lambda^2$. The far field distance for this horn array is also more than 50λ away from the horn apertures. This means that the near field effect of the feed must be considered in the analysis of our example antennas.

C Single-horn fed antennas

In this section, the single pyramidal horn designed in the previous section will be used as the feed of the dual-reflector antennas. The horn is firstly moved back and forth along the z_f axis in order to find a suitable position. Diffraction analysis is performed to compute the antenna efficiency for each trial position using conic reflector surfaces. It is found that the closer the horn aperture is to the subreflector, the higher the antenna efficiency. This is because the near field phase front of the horn does not substantially differ from the ideal spherical wavefront, and the spill-over loss is lessened with a shorter feed-to-subreflector distance. However, the horn



front view of
the 7-horn array

Figure 9: A 7-horn array feed.

can not be situated too close to the subreflector when feed blockage and the feed-subreflector interaction are considered. It is determined that the horn aperture be positioned at $z_f = 7\lambda$, which is about 8.5λ away from the subreflector. The near field right in front of the subreflector is plotted in Fig. 10. It can be observed that the amplitude distribution does not utilize the aperture in an efficient manner, and the wavefront differs from the ideal spherical one about $\pm 8^\circ$. The combination of these effects will produce low antenna efficiency and unsatisfactory antenna patterns if conic reflector surfaces are used. This is manifested by the PO far field patterns plotted in Fig. 11(a). These patterns suffer from loss of directivity, distorted side lobe structures and high asymmetry in the $\phi = 0^\circ$ and $\phi = 90^\circ$ planes. Notice that the PTD fringe field is not shown in these plots because in this region of observation the PO field is dominantly stronger and the effect of the fringe field can hardly be observed.

In order to compensate for the undesirable feed radiation characteristics and improve the antenna performances, the reflector surfaces will be shaped using the optimization mechanism described in a previous section. First of all, we leave the main reflector paraboloidal and shape the subreflector only. The resultant patterns are shown in Fig. 11(b). As can be seen, the patterns have been largely restored and the directivity has also been substantially improved. Next, we shape the main reflector and the subreflector simultaneously, and the results are shown in Fig. 11(c). These field patterns outperform those with only shaped subreflector by a better defined main beam region, sharper nulls and higher directivity. The results of reflector shaping using a single horn feed are summarized in Table 5, in which the effectiveness of reflector shaping can be readily observed.

As mentioned earlier, the extent of the SF₆ container is determined by the field

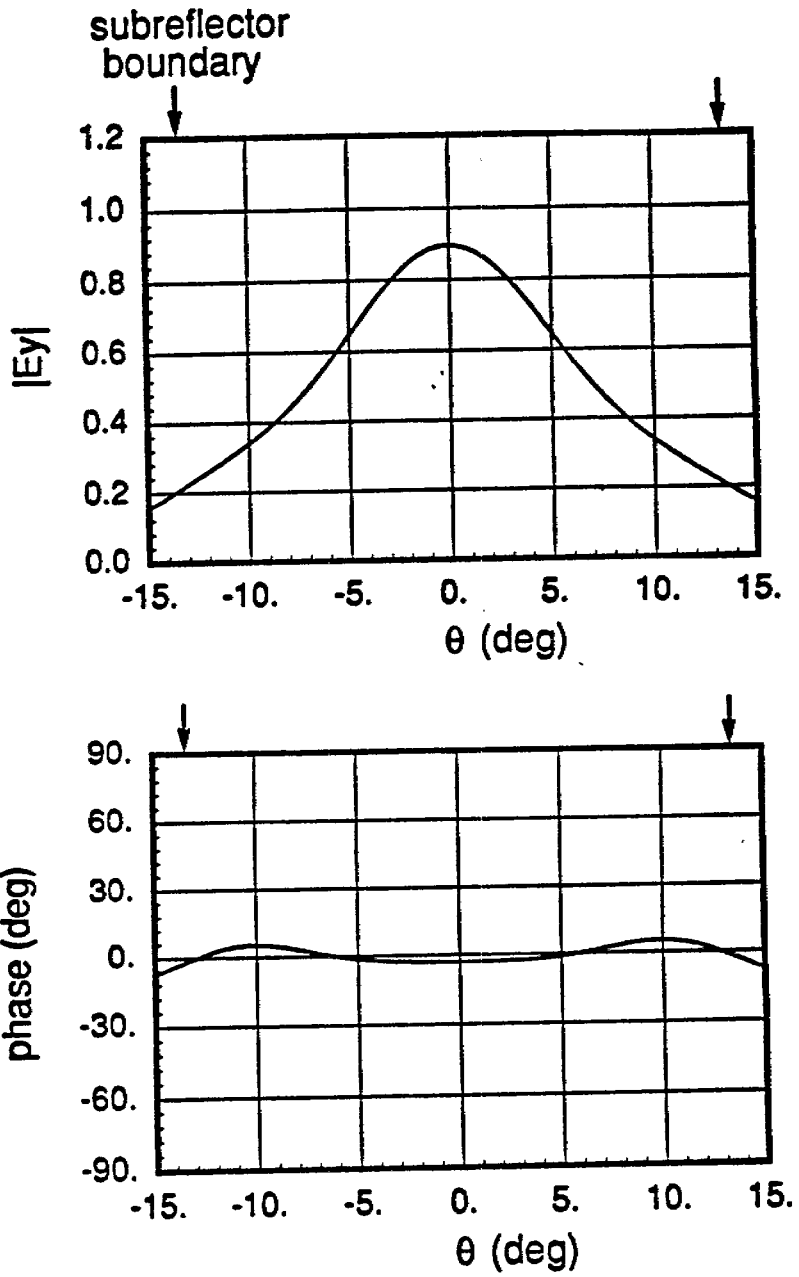


Figure 10: Near field of a single horn feed.

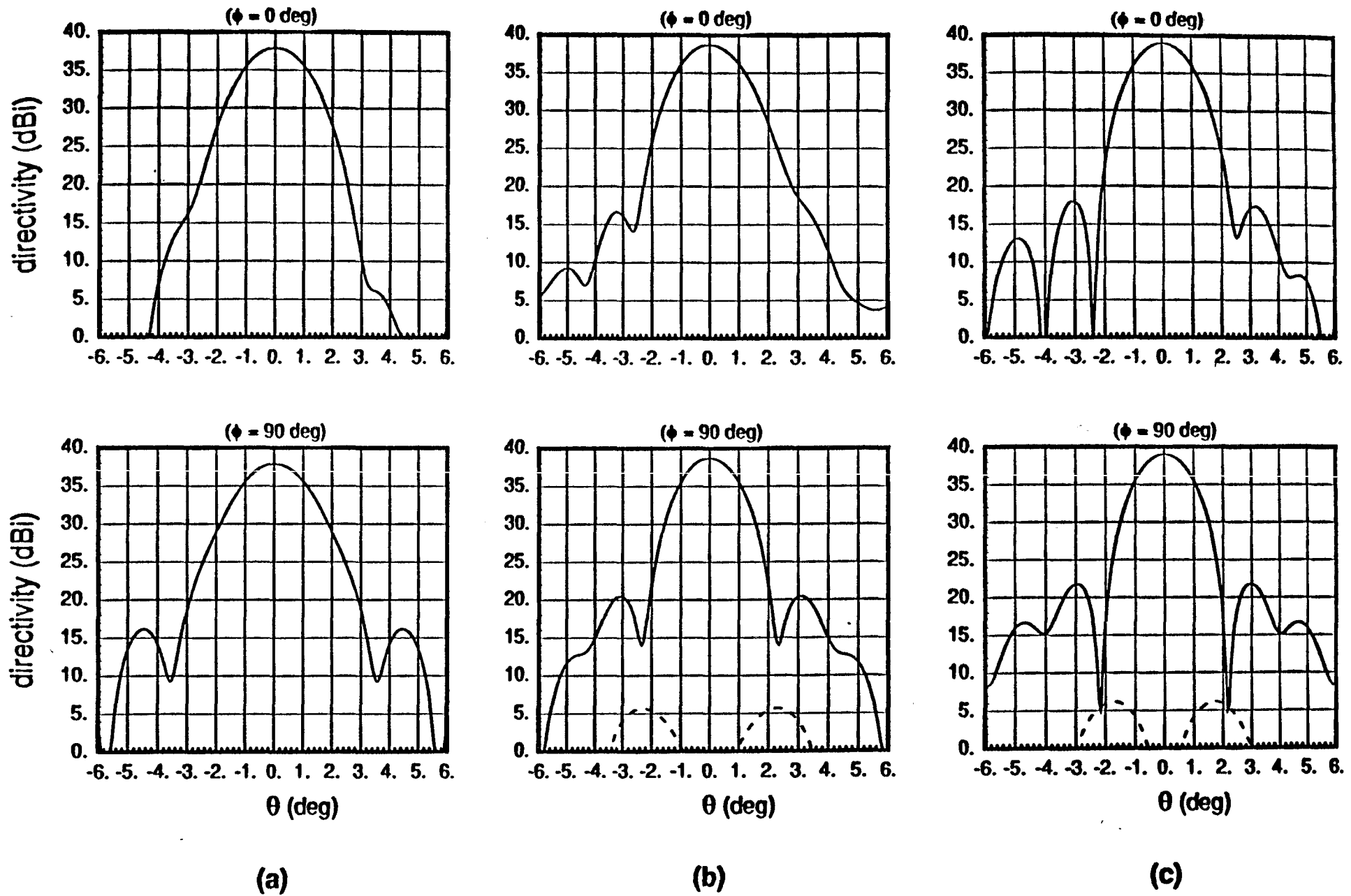


Figure 11: Far field patterns of single horn fed antennas using different main reflector/subreflector combinations. (a) paraboloidal/hyperboloidal. (b) paraboloidal/shaped. (c) shaped/shaped.

Table 5: Summary of antenna designs using a single-horn feed.

reflector types		boresight directivity	antenna efficiency
main	sub		
Paraboloidal	Hyperboloidal	37.9 dBi	57 %
Paraboloidal	Shaped	38.7 dBi	70 %
Shaped	Shaped	39.0 dBi	75 %

strength distribution. Therefore, it is important to be able to accurately predict the field strength in the near field of the antenna system in order to avoid the air breakdown problem. Determination of the near field strength can also be used to locate the safe range for personnel exposure. As a demonstration, the near fields of the single horn fed antenna that has both reflectors shaped are computed by the PO/PTD analysis, and the results are plotted in Fig. 12. Curves in Fig. 12 are plotted when the peak field in the horn aperture is 1 volts/m. To find the actual field strength at 1GW, 108.67 dB must be added to the field values read from this figure. It is obvious from this figure that the radiation from the subreflector and the feed must be included in order to obtain the actual total field strength, from which the extent of the SF₆ container can be determined. Notice that the interference pattern in the total field is resulted from the summation of complex-valued fields which have different time phases.

D Array-horn fed antennas

In this section, the 7-horn array will be used as the feed of the dual-reflector antennas. In order to avoid excessive spill-over loss, the horn array is placed at $z_f = 6.5\lambda$. The near field right in front of the subreflector is plotted in Fig. 13. It can be observed that the amplitude distribution is not well tapered, and the wavefront differs from the ideal spherical one almost $\pm 45^\circ$. This illumination is much worse than

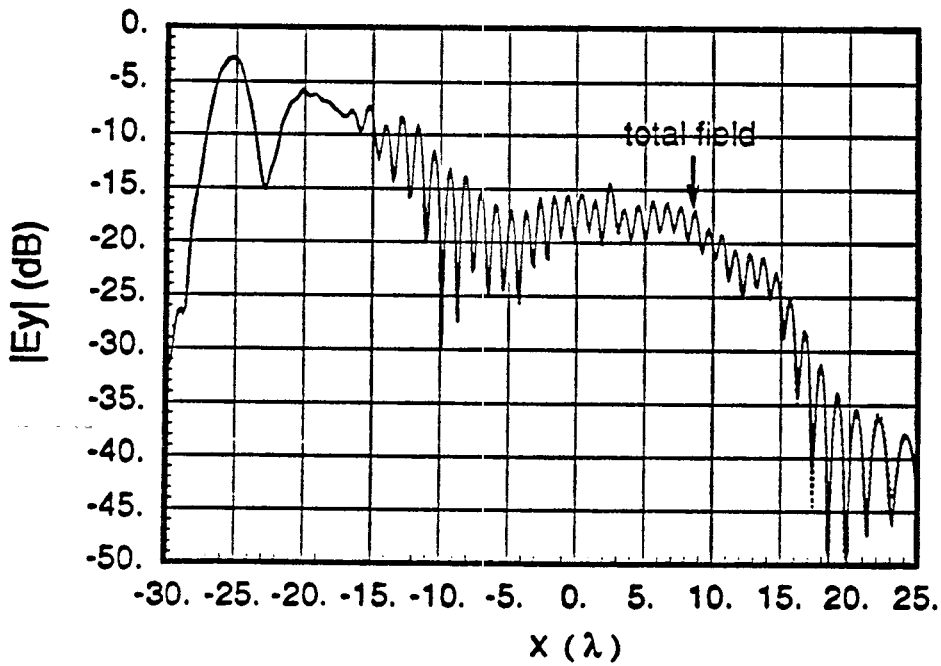
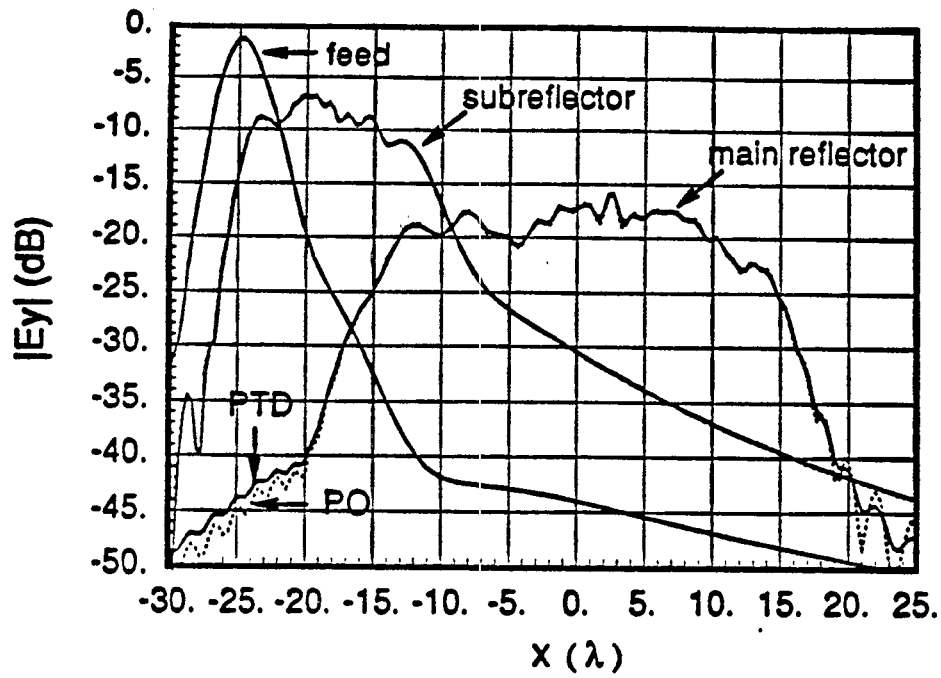


Figure 12: Normalized near field (at $z = -10\lambda$, $y = 0$ in Fig.6) of the single horn fed antenna that has both reflector surfaces optimally shaped. To find the actual field strength at 1 GW, 108.67 dB must be added to the field values read from this figure.

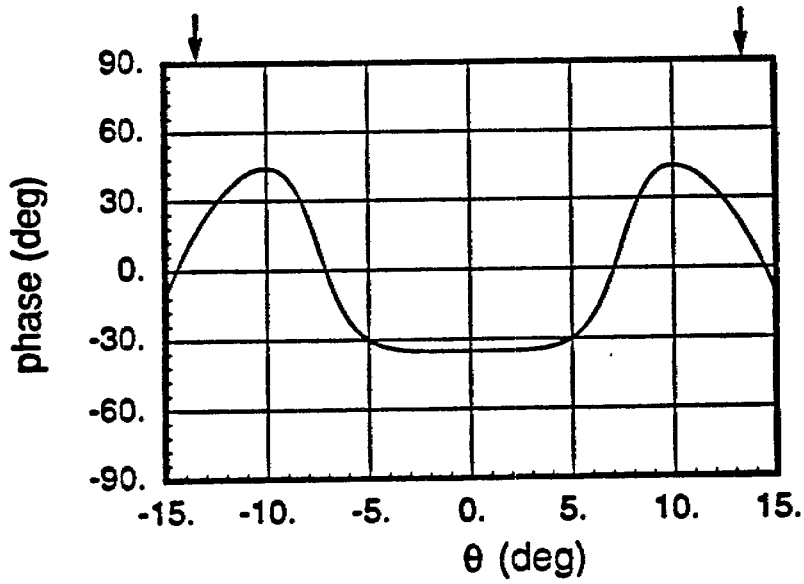
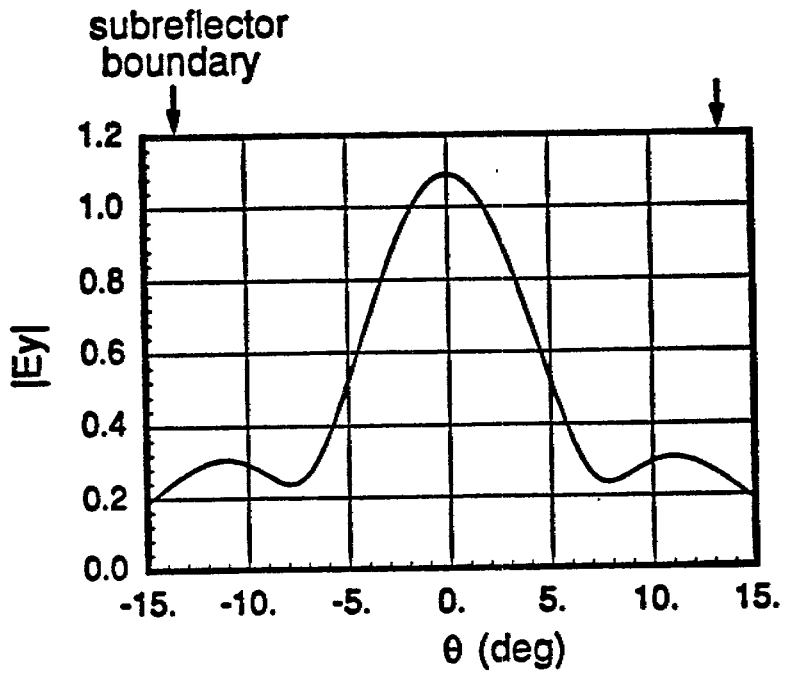


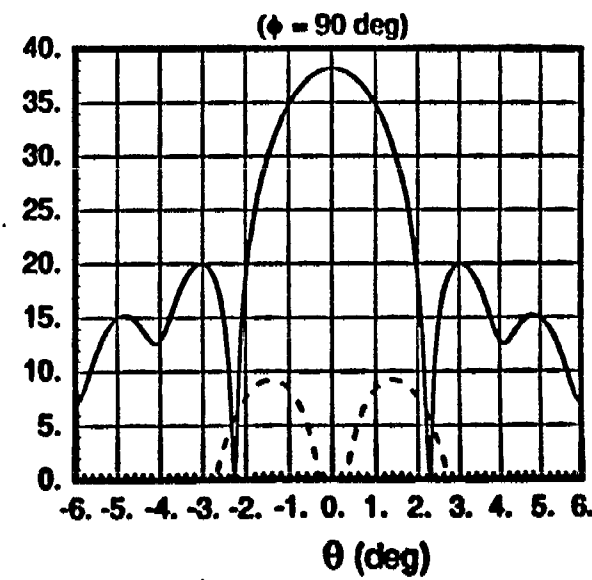
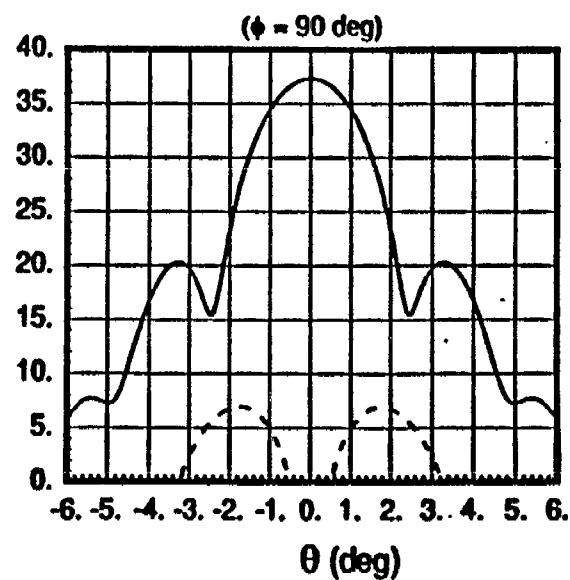
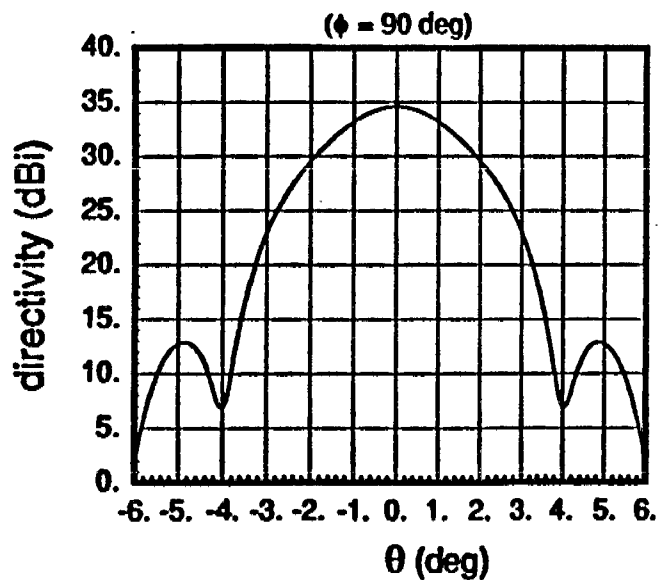
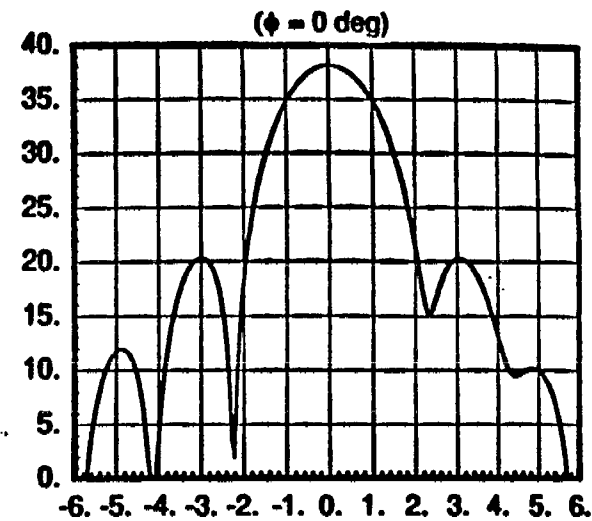
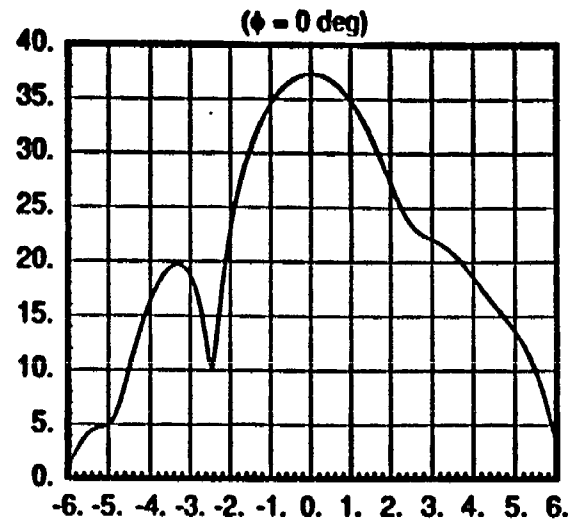
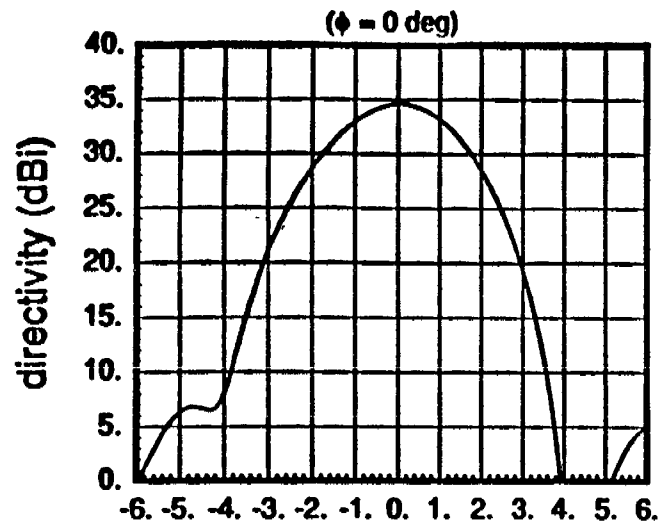
Figure 13: Near field of a 7-horn array feed.

Table 6: Summary of antenna designs using a 7-horn array feed.

reflector types		boresight directivity	antenna efficiency
main	sub		
Paraboloidal	Hyperboloidal	34.6 dBi	27 %
Paraboloidal	Shaped	37.3 dBi	50 %
Shaped	Shaped	38.2 dBi	61 %

that using a single horn feed. The unsatisfactory far field patterns are plotted in Fig. 14(a). These patterns have a very low directivity and badly distorted lobe structures.

In order to compensate for the feed illumination and improve the antenna performances, the reflector surfaces will be shaped using the optimization approach. It is important to mention that it is difficult to apply GO shaping algorithms to an array fed antenna. First of all, as in the single horn feed case, we leave the main reflector paraboloidal and shape the subreflector only. The resultant patterns are shown in Fig. 14(b). As can be seen, the patterns have been restored to a large extent and the directivity has also been substantially improved. Next, we shape the main reflector and the subreflector simultaneously, and the results are shown in Fig. 14(c). These field patterns outperform those with only shaped subreflector by a better defined main beam region, sharper nulls and higher directivity. The effectiveness of reflector shaping using optimization techniques for array fed antennas can be appreciated from Table 6, which summarizes the results of reflector shaping using a 7-horn array feed.



(a)

(b)

(c)

Figure 14: Far field patterns of 7-horn array fed antennas using different main reflector/subreflector combinations. (a) paraboloidal/hyperboloidal. (b) paraboloidal/shaped. (c) shaped/shaped.

VI Conclusion

Various radiating systems for generating HPM radiations were investigated. It was concluded that offset reflector antennas are suitable for these applications. The PO/PTD diffraction techniques were developed and applied to analyze both the main reflector and the subreflector in dual-reflector antennas that may use generally configured array feeds. The analysis results were presented with emphasis on both of the near and far field characteristics. An important design issue in designing HPM reflector antennas was that, in order to avoid air breakdown at high power levels, large horn aperture sizes and large element separations in array feeds were demanded. This resulted in poor spill-over efficiency and aperture efficiency. To overcome this difficulty, diffraction synthesis by optimization techniques was developed for designing HPM reflector antennas fed by single or array feeds. Design examples on reflector shaping in offset dual-reflector antennas were presented. The optimization approach was shown to be able to correct the undesired feed performance effectively. It was concluded that the general approach of PO/PTD analysis and optimization synthesis facilitate effective design and accurate characterization of HPM reflector antennas. The concepts and methodologies presented in this paper can be used to parameterly assess the high power performance and capabilities of any recommended reflector antenna systems.

References

- [1] R. E. Collin and F. J. Zucker, editors. "Antenna Theory, Parts 1 and 2". McGraw Hill, 1969.
- [2] Y. Rahmat-Samii. "Reflector antennas". In Y. T. Lo and S. W. Lee, editors, "Antenna Handbook", chapter 15. Van Nostrand Reinhold Company, New York, 1988.
- [3] C. E. Baum. "EMP simulators for various types of nuclear EMP". *IEEE Trans. EMC*, EMC-20:35-53, February 1978. Special issue on the nuclear electromagnetic pulse.
- [4] C. E. Baum. "Focused aperture antennas". Sensor and Simulation Notes 306, Air Force Weapons Laboratory, May 1987.
- [5] A. Michaeli. "Elimination of infinities in equivalent edge currents, part I: Fringe current components". *IEEE Trans. Antennas Propagat.*, AP-34(7):912-918, July 1986.
- [6] K. M. Mitzner. "Incremental length diffraction coefficients". Technical Report AFAL-TR-73-296, Aircraft Division Northrop Corp., April 1974.
- [7] M. Ando. "Radiation pattern analysis of reflector antennas". *Electronics and Communications in Japan, Part 1*, 68(4):93-102, 1985.
- [8] P. Y. Ufimtsev. "Method of edge waves in the physical theory of diffraction". *Izd-Vo Sovyetskoye Radio*, pages 1-243, 1962. Translation prepared by the U. S. Air Force Foreign Technology Division Wright-Patterson, AFB, Ohio (1971), available from NTIS, Springfield, VA22161, AD733203.
- [9] D. W. Duan, Y. Rahmat-Samii, and J. P. Mahon. "Scattering from a circular disc: a comparative study of PTD and GTD techniques". *Special issue of IEEE Proc. on Electromagnetics*, 1991. To be published.
- [10] D. G. Luenberger. "Linear and nonlinear programming". Addison-Wesley, 2nd edition, 1989.
- [11] J. E. Dennis, Jr. and R. B. Schnabel. "Numerical methods for unconstrained optimization and nonlinear equations". Computational mathematics. Prentice-Hall, 1983.
- [12] D. V. Giri. "Canonical examples of high-power (HPM) radiation systems for the case of one feeding waveguide". Sensor and Simulation Notes 326, Air Force Weapons Laboratory, April 1991.